

Magnetic and magnetoelastic properties in tetragonal TbPO₄

P. Morin and J. Rouchy

Laboratoire Louis Néel, CNRS, 166X, 38042 Grenoble Cedex, France

Z. Kazei

Laboratory for Magnetism, Physics Department, Moscow State University, 119899 Moscow, Russia

(Received 15 April 1994; revised manuscript received 31 May 1994)

The magnetic and magnetoelastic properties (third-order magnetic susceptibility and parastriction) of TbPO₄, which has the zircon-type tetragonal structure, are analyzed in the paramagnetic phase. The susceptibility formalism is then used to describe all the symmetry-lowering modes in a rare-earth insulator. The dominant magnetoelastic coupling is associated with the δ symmetry and is, at least partly, responsible for the transition occurring at 2.15 K in the antiferromagnetic phase and clearly dominates the γ -symmetry mode. However, none of the different symmetry-lowering modes can be completely neglected and we determine parameters for the $\alpha 1$ and $\alpha 2$ tetragonal modes and the ϵ monoclinic mode. Owing to the close vicinity of the first excited singlet to the ground-state doublet, the α quadrupolar interactions play an important role in determining the temperature dependence of the level spacing at low temperature, in particular in the ordered phases. The determination of all the magnetoelastic modes of TbPO₄ is an essential step towards the understanding of the complex magnetic properties in the ordered phases, where numerous interactions coexist.

I. INTRODUCTION

For the past 25 years, vanadates and phosphates of rare earths with tetragonal zircon-type structure have motivated a great number of studies of the Jahn-Teller coupling. Thus TmVO₄ and some other vanadates are now atypical examples of quadrupolar ordering of magnetoelastic origin.^{1,2} RPO₄ compounds (*R* is a heavy rare earth) differ from the vanadates due essentially to peculiarities in their magnetocrystalline anisotropy. The main difference is that the second-order crystalline electric-field (CEF) parameter V_2^0 has an opposite sign, with the obvious consequence that the anisotropy between the *c* axis and the basal plane is inverted.³ However, another important difference is that RPO₄ compounds do not have structural transitions in the paramagnetic phase, which follows from the particular CEF mixing of the eigenfunctions of their low-lying levels, although the magnetoelastic couplings remain as large as in isomorphous RVO₄ compounds.⁴ Among the phosphates, TbPO₄ in particular has motivated many experimental studies (only a few of the most recent ones are referred to here), with respect to its CEF properties,⁵⁻⁷ as well as its low-temperature properties in ordered phases.⁸⁻¹⁶ TbPO₄ orders antiferromagnetically at 2.28 K with collinear moments pointing along the *c* axis,¹⁰ and very close to T_N , at 2.13 K, a change in the magnetic structure is observed, manifested as a tilt of the moments away from the *c* axis in the (-110) plane. The tilt angle seems to be temperature dependent¹¹ and to reach around 20° at 1.5 K.¹⁰ This tilt of the moments is accompanied by a symmetry lowering to a structure which is probably monoclinic.

The analysis of magnetic properties in ordered phases

leaves some unanswered questions. Although the fact that the change of the anisotropy in the (-110) plane can be explained in terms of dominant quadrupolar interactions within the δ symmetry, the value of the tilt angle itself cannot be explained: indeed, in a tetragonal cell sheared along the [110] axis, the easy magnetization direction remains along a high-symmetry direction, i.e., the [001] or [110] axes of the high-temperature tetragonal phase. In order to explain an in-plane intermediate moment direction, one needs to consider either the contribution of the ϵ mode (shearing of the plane) or additional couplings besides the harmonic elasticity. To improve our understanding of TbPO₄, we therefore start with the study of the various magnetoelastic modes.

For such an approach, the susceptibility formalism for magnetic and magnetoelastic properties is a powerful tool. Indeed, a possible criticism which might be made against the previous studies is that the quantum treatment dictated by the CEF mixing of the eigenfunctions, despite being properly applied for analyzing light-scattering results and determining low-lying levels, has generally been forsaken in favor of less fundamental pseudospin methods when it comes to the description of the magnetic and magnetoelastic properties. The continued application of the quantum treatment allows additional understanding of the level schemes in terms of the fundamental couplings, which may then be compared across a series (here RPO₄ and RVO₄).

Such a quantum formalism has allowed an analysis of the magnetic and quadrupolar properties in cubic and tetragonal rare-earth intermetallics.¹⁷ In addition to the treatment in the disordered phase of the first-order magnetic susceptibility and of the strain susceptibility for the elastic constant softening, it can describe parastriction

processes and direct effects of the quadrupolar interactions on the third-order magnetic susceptibility. Through different coherent studies, quadrupolar orderings are now fully explained as, for instance, in TmZn and TmCd. The impact of quadrupolar interactions in the ordered phase is also well understood, at least in cubic intermetallics.¹⁸ Tetragonal TmAg₂ is a perfect archetype for quadrupolar ordering driven by pair interactions,¹⁹ and allows comparisons with *R* tetragonal insulators. Indeed, a classification may be proposed that quadrupolar ordering can be induced either by magnetoelastic coupling only, as in insulators, or by pair interactions (not systematically related to the phonon coupling, if mediated by conduction electrons). When pair interactions are positive, they stabilize the same type of ferroquadrupolar order as the magnetoelastic coupling. The best evidence of this order is the symmetry lowering associated with the (nonzero) magnetoelastic coupling, through a kind of quadrupolar striction.²⁰ When negative, they may induce, in competition with magnetoelasticity, an antiferroquadrupolar arrangement as observed in CeB₆ and recently in UPd₃.²¹ Thus a quantitative comparison of the different quadrupolar couplings between rare-earth insulators and intermetallics may be quite illustrative.

After recalling the magnetic and quadrupolar susceptibility formalism (Sec. II) and discussing the CEF coupling (Sec. III), our present aim is to check the formalism's efficiency in the case of TbPO₄ by determining all the magnetoelastic couplings (Secs. IV and V). The results will be discussed in Sec. VI.

II. FORMALISM

The magnetic properties of the *4f* shell are described for a tetragonal symmetry using the following Hamiltonian within the mean-field approximation (MFA):²²

$$\mathcal{H} = \mathcal{H}_{\text{CEF}} + \mathcal{H}_M + \mathcal{H}_{\text{ME}} + \mathcal{H}_Q + E_{\text{el}} + E_M + E_Q. \quad (1)$$

The CEF term \mathcal{H}_{CEF} is written using the operator equivalent method²³ within a system of *x*, *y*, and *z* axes parallel to the [110], [010], and [001] axes of the lattice cell, respectively:

$$\begin{aligned} \mathcal{H}_{\text{CEF}} = & \alpha_J V_2^0 O_2^0 + \beta_J (V_4^0 O_4^0 + V_4^4 O_4^4) \\ & + \gamma_J (V_6^0 O_6^0 + V_6^4 O_6^4). \end{aligned} \quad (2)$$

O_1^m are the Stevens operators, V_1^m the CEF parameters, and α_J , β_J , and γ_J the Stevens coefficients. The magnetic terms in \mathcal{H}_M are the Zeeman coupling to the applied magnetic field, \mathbf{H} , corrected for demagnetizing effects and the Heisenberg-type bilinear interactions, characterized by a θ^* magnetic interaction temperature. Only magnetoelastic contributions linear in strain and restricted to second-rank terms are considered here. They read in symmetrized notation as²⁴

$$\begin{aligned} \mathcal{H}_{\text{ME}} = & -(B^{\alpha 1} \varepsilon^{\alpha 1} + B^{\alpha 2} \varepsilon^{\alpha 2}) O_2^0 - B^\gamma \varepsilon^\gamma O_2^2 - B^\delta \varepsilon^\delta P_{xy} \\ & - B^\varepsilon (\varepsilon_1^\varepsilon P_{zx} + \varepsilon_2^\varepsilon P_{yz}). \end{aligned} \quad (3)$$

The B^μ 's are the magnetoelastic coefficients. The related elastic energy is

$$\begin{aligned} E_{\text{el}} = & \frac{1}{2} C_0^{\alpha 1} (\varepsilon^{\alpha 1})^2 + C_0^{\alpha 12} \varepsilon^{\alpha 1} \varepsilon^{\alpha 2} + \frac{1}{2} C_0^{\alpha 2} (\varepsilon^{\alpha 2})^2 \\ & + \frac{1}{2} C_0^\gamma (\varepsilon^\gamma)^2 + \frac{1}{2} C_0^\delta (\varepsilon^\delta)^2 + \frac{1}{2} C_0^\varepsilon [(\varepsilon_1^\varepsilon)^2 + (\varepsilon_2^\varepsilon)^2]. \end{aligned} \quad (4)$$

The ε^μ strains and the C_0^μ lattice background elastic constants are given in Table I. Within the MFA, the two-ion quadrupolar terms are written as

$$\begin{aligned} \mathcal{H}_Q = & -K^\alpha \langle O_2^0 \rangle O_2^0 - K^\gamma \langle O_2^2 \rangle O_2^2 - K^\delta \langle P_{xy} \rangle P_{xy} \\ & - K^\varepsilon [\langle P_{yz} \rangle P_{yz} + \langle P_{zx} \rangle P_{zx}]. \end{aligned} \quad (5)$$

E_Q and E_M in Eq. (1) are the quadrupolar and bilinear corrective energies associated with the MFA. Minimizing the free energy with regard to the strains gives the equilibrium strains as functions of the expectation values of the corresponding quadrupolar operators. Replacing these ε^μ 's makes \mathcal{H}_{ME} [Eq. (3)] indistinguishable from \mathcal{H}_Q [Eq. (5)] and leads to total quadrupolar coefficients:

$$G^\mu = \frac{(B^\mu)^2}{C_0^\mu} + K^\mu \quad (\mu = \gamma, \delta, \varepsilon) \quad (6)$$

and

$$G^\alpha = \frac{(B^{\alpha 1})^2 C_0^{\alpha 2} - 2B^{\alpha 1} B^{\alpha 2} C_0^{\alpha 12} + (B^{\alpha 2})^2 C_0^{\alpha 1}}{C_0^{\alpha 1} C_0^{\alpha 2} - (C_0^{\alpha 12})^2} + K^\alpha. \quad (6')$$

The complicated expression of G^α comes from the existence of two α magnetoelastic modes.²² Note that in tetragonal symmetry, the O_2^0 component is already ordered by the CEF. In the absence of any external stress or magnetic field, Eq. (1) reduces to $\mathcal{H}_{\text{CEF}} - G^\alpha \langle O_2^0 \rangle O_2^0$.

TABLE I. Symmetrized strains and elastic constants in tetragonal symmetry.

Representations	Strains	Elastic constants
Γ_1	$\varepsilon^{\alpha 1} = \frac{1}{\sqrt{3}} (\varepsilon_{xx} + \varepsilon_{yy} + \varepsilon_{zz})$	$C^{\alpha 1} = \frac{1}{3} (2C_{11} + 2C_{12} + 4C_{13} + C_{33})$
Γ_1	$\varepsilon^{\alpha 2} = \left(\frac{2}{3}\right)^{1/2} \left[\varepsilon_{zz} - \frac{\varepsilon_{xx} + \varepsilon_{yy}}{2} \right]$	$C^{12} = -\frac{\sqrt{2}}{3} (C_{11} + C_{12} - C_{13} - C_{33})$ $C^{\alpha 2} = \frac{1}{3} (C_{11} + C_{12} - 4C_{13} + 2C_{33})$
Γ_3	$\varepsilon^\gamma = \frac{1}{\sqrt{2}} (\varepsilon_{xx} - \varepsilon_{yy})$	$C^\gamma = C_{11} - C_{12}$
Γ_4	$\varepsilon^\delta = \sqrt{2} \varepsilon_{xy}$	$C^\delta = 2C_{66}$
Γ_5	$\varepsilon_1^\varepsilon = \sqrt{2} \varepsilon_{zx}$	$C^\varepsilon = 2C_{44}$
	$\varepsilon_2^\varepsilon = \sqrt{2} \varepsilon_{yz}$	

This leads to an apparent second-order CEF coefficient, which is temperature dependent through the thermal variation of $\langle O_2^0 \rangle$ and thus to a level scheme which is also temperature dependent. The G^α term then has to be considered in addition to the CEF *ab initio* before the diagonalization which leads to the eigenfunctions and energy levels. It is unknown at this initial step, but may be determined by an analysis of the parastriction induced by a field and reintroduced into the initial diagonalization in a kind of self-consistent loop.

In insulating systems, the two-ion quadrupolar terms originate from electric quadrupole-quadrupole interactions and phonon coupling.^{1,2} The second term is dominant and receives contributions from both optical and acoustic phonons. The acoustic contribution to K^μ is negative, and a relation between the pair interaction coefficient K^μ and the magnetoelastic contribution to G^μ , $G_{ME}^\mu = (B^\mu)^2 / C_0^\mu$ is then deduced: $K^\mu / G_{ME}^\mu = -\frac{1}{3}$. This ratio is close to that observed, for instance, in TmPO_4 , and also appears as a general feature for rare-earth zircons.^{1,2,20} Owing to the dominant long-wavelength acoustic contribution to Eq. (5), the mean-field theory works well and allows development following the susceptibility formalism.

Indeed, in the presence of small external stresses, perturbation theory can be applied very fruitfully to the disordered phase. It is then possible to obtain analytical expressions for the free energy associated with each of the symmetry-lowering modes and then to describe the corresponding couplings. Calculations are detailed in Ref. 22. For example, the third-order magnetic susceptibility, i.e., the initial curvature of the magnetization curve

$$\chi_M^{(3)} = \frac{1}{\left[1 - \frac{\theta^*}{C} \chi_0\right]^4} \left[\chi_0^{(3)} + \frac{2G^\alpha (\chi_\alpha^{(2)})^2}{1 - G^\alpha \chi_\alpha} + \frac{2G^\mu (\chi_\mu^{(2)})^2}{1 - G^\mu \chi_\mu} \right], \quad (7)$$

depends on four single-ion susceptibilities (C is the Curie constant): χ_0 is the single-ion susceptibility, anisotropic between the [001] axis and the basal plane; $\chi_0^{(3)}$ describes the curvature of the magnetic response in the absence of any magnetic interaction. The strain susceptibility $\chi_\mu = \partial \langle O_2^\mu \rangle / \partial \epsilon^\mu$ characterizes the response of the Q_μ quadrupolar component to the associated strain, and $\chi_\mu^{(2)} = \partial \langle O_2^\mu \rangle / \partial H^2$ is the equivalent with respect to an applied magnetic field. The anisotropic $\chi_0^{(3)}$'s, χ_μ 's and $\chi_\mu^{(2)}$'s are deduced immediately from the CEF levels and eigenfunctions.

The strains induced in the disordered phase by a magnetic field applied along a $(\alpha_1 \alpha_2 \alpha_3)$ direction,

$$\epsilon^\mu = \frac{B^\mu}{C_0^\mu} \frac{\chi_\mu^{(2)}}{\left[1 - \frac{\theta^*}{C} \chi_0\right]^2 (1 - G^\mu \chi_\mu)} H^2, \quad (8)$$

contribute to the change of length measured in the

$(\beta_1 \beta_2 \beta_3)$ direction,

$$\begin{aligned} \lambda_{\alpha_1 \alpha_2 \alpha_3}^{\beta_1 \beta_2 \beta_3} &= \left[\frac{\delta l}{l} \right]_{\alpha_1 \alpha_2 \alpha_3}^{\beta_1 \beta_2 \beta_3} \\ &= \frac{\epsilon^{\alpha 1}}{\sqrt{3}} + \frac{1}{\sqrt{6}} \epsilon^{\alpha 2} (2\beta_3^2 - \beta_1^2 - \beta_2^2) + \frac{1}{\sqrt{2}} \epsilon^{\alpha 3} (\beta_1^2 - \beta_2^2) \\ &\quad + \sqrt{2} \epsilon^\delta \beta_1 \beta_2 + \sqrt{2} \beta_3 (\epsilon_1^\epsilon \beta_1 + \epsilon_2^\epsilon \beta_2). \end{aligned} \quad (9)$$

Extensive applications of the susceptibility formalism in tetragonal symmetry can be found in Ref. 19 for TmAg_2 .

From an experimental point of view, the initial step requires a knowledge of the CEF, which determines single-ion susceptibilities. The fit of the first-order magnetic susceptibility along the [001] axis and in the basal plane provides us with the bilinear coefficient θ^* . The third-order magnetic susceptibility and parastriction subsequently give different pairs of B^μ and K^μ coefficients. This process is developed in the following sections, unfortunately without the third experimental probe to determine the B^μ 's and K^μ 's, i.e., the elastic constants; indeed we failed to measure them and there is no corresponding data for TbPO_4 in the literature.

III. THE CRYSTALLINE ELECTRIC FIELD

An initial set of CEF parameters is provided by very careful light-scattering experiments done by Böhm, Kahle, and Wüchner.⁶ J mixing was considered when analyzing absorption spectra collected at temperatures ranging from 2.3 to 20 K in applied magnetic fields up to 4 T. Emission spectra were also collected at various temperatures. The analysis leads to a rather complex level scheme with a ground-state doublet and an excited singlet around 3.6 K, a second singlet at 13.7 K and a third one at 29.8 K. Other levels are observed ranging from 120 up to 380 K. Calculations considering the only 7F_6 multiplet showed that the energies of the lowest levels depend most sensitively on small changes in the V_1^m parameters, whereas the corresponding wave functions are practically unchanged. The deduced parameters were $V_2^0 = 253$ K, $V_4^0 = 20$ K, $V_4^4 = 1277$ K, $V_6^0 = -72$ K, and $V_6^4 = -153$ K (set 1), here expressed in relation to our system of axes (see Sec. II). However, this set of CEF parameters was reported not to describe very well the transfers observed around 80–90 cm^{-1} .

Our calculations, also considering only the ground-state multiplet, are in full agreement with previous ones. Starting from the spacings and wave functions given in Table 2 of Ref. 6, we then tried to estimate the volume surrounding the previous set of values in the superspace of the parameters. Indeed, it may be important to check the influence of small shifts of the V_1^m 's on the various susceptibilities used in the analyses of magnetic and magnetostriction data. Set 1 does not appear unique, as shown in Table II, where another set, set 2, is proposed, which leads to a slightly smaller residue. The main differences between the two schemes are that, in set 2, the V_4^0 value is twice as large and the V_4^4 parameters are both positive. However, the various CEF susceptibilities deduced with the two sets of V_1^m 's are very similar, except

TABLE II. Spacings from the ground-state doublet observed by light spectroscopy (first line) and calculated according to set 1 (second line) and set 2 (third line), defined by $V_2^0=266$ K, $V_4^0=37$ K, $V_4^4=1246$ K, $V_6^0=-52$ K, and $V_6^4=126$ K. Underlined values correspond to spacings for doublets.

$\Delta_{ij}(K)$	3.6	13.7	29.8	115	<u>125</u>	366	<u>377</u>		
exper.	± 1.4	± 0.7	± 1.4	± 7	± 7	± 12	± 12		
calc.	2.91	15.13	35.81	137.62	<u>138.92</u>	146.32	359.27	<u>373.54</u>	386.40
Set 1									
calc.	4.42	12.17	31.84	117.61	<u>122.57</u>	128.32	360.13	<u>373.43</u>	385.41
Set 2									

at very low temperatures, i.e., in the ordered range or a few K above T_N . This implies that only the analysis of the properties in the ordered phase (which is out of the scope of the present study) would depend on the starting CEF parameters. All the following calculations in the paramagnetic phase will be presented using set 1 from Ref. 6, although results have been systematically checked using set 2.

IV. MAGNETIC SUSCEPTIBILITIES

The isothermal magnetization curves were obtained along the [001], [100], and [110] directions in fields up to 76 kOe for temperatures ranging from 1.5 to 300 K. The susceptibility values were then deduced in vanishing field from $M/H(H^2)$ plots. Along the [110] axis, the magnetization curve exhibits a smooth S shape; such a behavior was previously observed in the disordered phases of TmZn (Ref. 17) and TmAg₂,¹⁹ and was explained by a sudden increase of the quadrupolar structure under field. The field value of the corresponding inflection point decreases at low temperatures: therefore, in order to avoid possible residual magnetostrictive strains from one isothermal field variation to the next, the maximum field value was lowered and the sample warmed up to 150 K between two isothermal field variations. Within the experimental accuracy, the magnetic susceptibility is isotropic in the basal plane, as expected for the tetragonal symmetry.

A. First-order magnetic susceptibility

The temperature variations of the reciprocal susceptibility are drawn in Fig. 1. Note that at high temperature, the two curves are not parallel, which indicates CEF contributions are still active. Set 1 gives a good fit to these data using a bilinear interaction temperature $\theta^* = -3.2$ K. Set 2 does not give any improvement, except perhaps below 20 K along the c axis of easy magnetization, where the improvement is of marginal statistical significance. A third scheme was proposed by Sen, Neogy, and Wanklyn ($V_2^0=257$ K, $V_4^0=23$ K, $V_4^4=1306$ K, $V_6^0=-76$ K, and $V_6^4=-161$ K), as a fit to both light scattering transfers and magnetic susceptibility.⁷ It also fits our first-order susceptibility data well with the same rms deviation in the entire investigated range (the rms deviation is slightly smaller when limiting the temperature range below 50 K). In the following, the $\theta^* = -3.2$ K coefficient will be kept constant.

B. Third-order magnetic susceptibility

The third-order magnetic susceptibility is given by the slope of the linear part of $M/H(H^2)$. The $\chi_M^{(3)}$ temperature dependences are drawn in Fig. 2. Along the [110] axis, the $\chi_M^{(3)}$ data are positive, contrary to the values calculated without quadrupolar interactions in the thermal range investigated. Consideration of the negative bilinear interactions only reduces the absolute value of the third-order susceptibility. Quadrupolar interactions characterized by $G^\delta=90$ mK drive the calculated variation to be positive and close to the experimental one. The possible contribution [see Eq. (7)] of quadrupolar interactions within the α symmetry are not considered here, and will be discussed later. Along the [100] axis, the third-order susceptibility is negative down to 3.5 K, the temperature at which it changes sign. The data are quite correctly described down to 4.5 K when including bilinear interactions. The third-order susceptibility is not significantly sensitive to quadrupolar interactions within the γ sym-

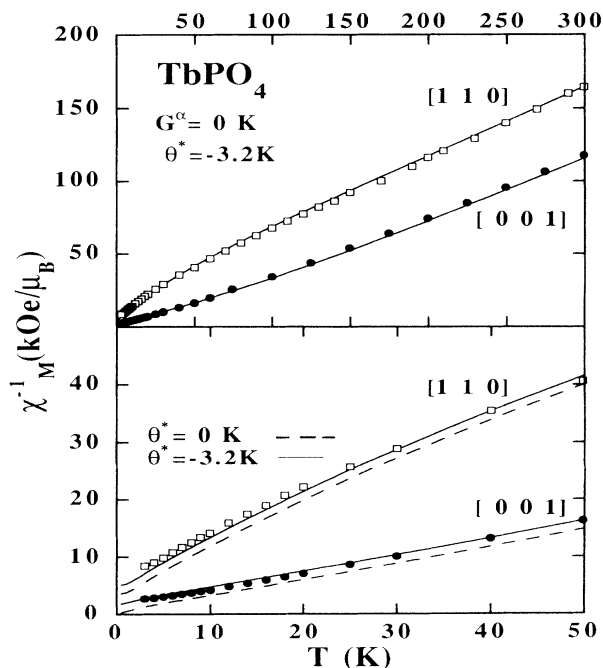


FIG. 1. The temperature dependence of the reciprocal first-order susceptibility along the [001] (data: full dots) and [110] (data: open dots) axes with and without bilinear interactions (full and hatched lines, respectively).

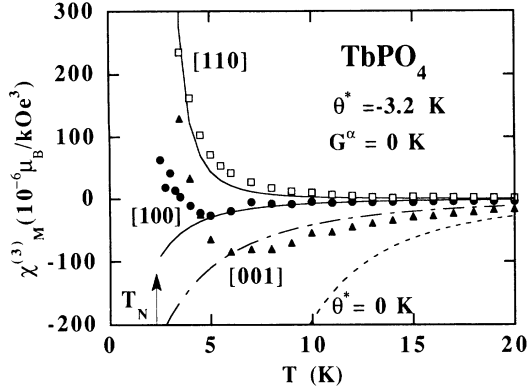


FIG. 2. The temperature variation of the third-order susceptibility along the main crystallographic directions ([110] data: open squares, [100] data: black dots and [001] data: triangles). Curves are calculated with bilinear interactions characterized by $\theta^* = -3.2$ K, except the hatched one, which is calculated for $\theta^* = 0$ K along the c axis. Quadrupolar interactions are only present for the δ symmetry ($G^\delta = 90$ mK; see text).

metry. Thus the upward behavior between 4.5 K and T_N cannot be driven by quadrupolar interactions and may be due to short-range order. Along the [001] axis of easy magnetization, the third-order susceptibility is negative as expected for a magnetic doublet as the ground state.²² As along the [100] direction, an upward variation toward positive values is observed around 6 K and can also be associated with short-range effects. Note that this behavior is reminiscent of the positive curvature, standard for temperatures below an antiferromagnetic transition. The fit with $\theta^* = -3.2$ K is not perfect; it would be improved for a value around -2.5 K. The effects of the α -symmetry quadrupolar interactions will be discussed later.

V. PARASTRICTION MEASUREMENTS

Magnetostriction data have been collected with strain gauges in field up to 5 T and in temperatures from 1.5 to 250 K. The sensitivity is limited to around 10^{-7} . The magnetic field was applied successively parallel to the [100], [110], [001], and [101] crystallographic directions. In each case, gauges were glued along the [100], [010], and [001], [110] and $[-110]$, [001] and [100], [101] and $[-101]$ directions, respectively. Shortened notations for the changes of length [see Eq. (9)] are used in the following: $\lambda_{ij} = \lambda_{\alpha_1 \alpha_2 \alpha_3}^{\beta_1 \beta_2 \beta_3}$. The first subscript i corresponds to the gauge direction, the second one j to the field direction ($i, j = a \equiv [100]$, $a' \equiv [010]$, $b \equiv [110]$, $b' \equiv [-110]$, and $c \equiv [001]$). The data are plotted against the square of the field (Fig. 3). The range of linearity depends both on the temperature and the normal strain modes present. Linear combinations then lead to the normal modes. The temperature dependence of their initial slope has then to be compared to predictions from the susceptibility formalism.

A. The α mode

This mode is usually smaller than the symmetry-lowering modes, as observed, for instance, in TmAg_2 ,¹⁹

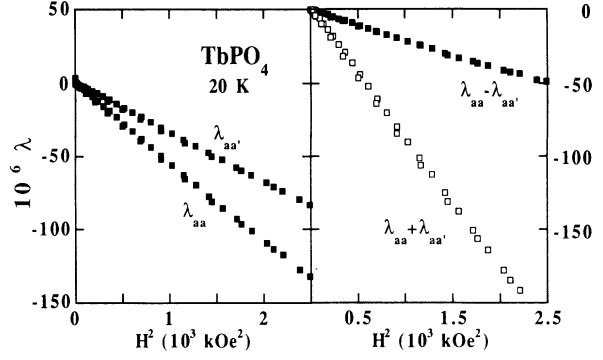


FIG. 3. Changes of length as functions of the square of the magnetic field at 20 K, parallel (λ_{aa}) and perpendicular ($\lambda_{aa'}$) to the [100] direction of the applied field (left part). Variations deduced for the γ strain, ($\lambda_{aa} - \lambda_{aa'}$), and the ($\lambda_{aa} + \lambda_{aa'}$) contribution to the α modes (right part).

and thus is often neglected. As it concerns the $\langle O_2^0 \rangle$ quadrupolar component already ordered by the CEF, and as it consists of two contributions (bulk variation and change of the c/a ratio), it is also more difficult to study thoroughly. It is observed here under two experimental conditions, H parallel to the [001] and [100] directions. From λ_{cc} , λ_{ac} , λ_{aa} , $\lambda_{aa'}$, and λ_{ca} , according to Eq. (8) one obtains thermal variations linearized at least at high temperature:

$$\frac{H}{\sqrt{|\lambda_{cc} - \lambda_{ac}|}} = \sqrt[4]{\frac{2}{3}} \frac{1}{\sqrt{|A^{a2}|}} \frac{1}{\sqrt{|\chi_\alpha^{(2)}|}} (1 - n\chi_0) \times (1 - G^\alpha \chi_\alpha)^{1/2}, \quad (10)$$

$$\frac{H}{\sqrt{|\lambda_{cc} + 2\lambda_{ac}|}} = \sqrt[4]{\frac{1}{3}} \frac{1}{\sqrt{|A^{a1}|}} \frac{1}{\sqrt{|\chi_\alpha^{(2)}|}} (1 - n\chi_0) \times (1 - G^\alpha \chi_\alpha)^{1/2} \quad (10')$$

for H parallel to [001], and

$$\frac{H}{\left| \left| \lambda_{ca} - \frac{\lambda_{aa} + \lambda_{aa'}}{2} \right| \right|^{1/2}} = \sqrt[4]{\frac{2}{3}} \frac{1}{\sqrt{|A^{a2}|}} \frac{1}{\sqrt{|\chi_\alpha^{(2)}|}} \times (1 - n\chi_0)(1 - G^\alpha \chi_\alpha)^{1/2}, \quad (11)$$

$$\frac{H}{\sqrt{|\lambda_{ca} + \lambda_{aa} + \lambda_{aa'}|}} = \sqrt[4]{\frac{1}{3}} \frac{1}{\sqrt{|A^{a1}|}} \frac{1}{\sqrt{|\chi_\alpha^{(2)}|}} \times (1 - n\chi_0)(1 - G^\alpha \chi_\alpha)^{1/2} \quad (11')$$

for H parallel to [100]. A^{a1} and A^{a2} depend on both the background elastic constants and the magnetoelastic coefficients:

$$A^{a1} = \frac{B^{a1} C_0^{a2} - B^{a2} C_0^{a12}}{C_0^{a1} C_0^{a2} - (C_0^{a12})^2}$$

and

$$A^{a2} = \frac{B^{a2} C_0^{a1} - B^{a1} C_0^{a12}}{C_0^{a1} C_0^{a2} - (C_0^{a12})^2}.$$

Note that the ratio of Eqs. (10) and (11) are equal to the same constant $2^{1/4}(A^{\alpha 1}/A^{\alpha 2})^{1/2}$.

The experimental temperature variations are drawn in Fig. 4. The best accuracy is obtained for the c axis data, due to the fact that this is less sensitive to misorientations of the field and the gauge than for a direction within the basal plane. For the two field orientations [100] and [001], the ratio of the slopes relative to the $\alpha 1$ and $\alpha 2$ modes is equal to 1.4, which proves the coherency of the determinations.²⁵

The fit to the data using Eqs. (10) and (11) leads, within experimental accuracy, to $A^{\alpha 1}=3.2 \times 10^{-5}$ and $A^{\alpha 2}=-4.7 \times 10^{-5}$. Some discrepancies are present only at low temperature, say below 7 K. Note the divergence of the calculated variations around 5 and 2 K for H parallel to [100] and [001], respectively. The corresponding vanishing of the α strains depends on the exact characteristics of the level spacing at low temperature: for instance, it is calculated to be absent along [001] with sets 2 and 3 and, from an experimental point of view, it may be hidden by short-range ordering. Another reason for the discrepancy to the data may be the feedback of these α quadrupolar interactions on the level scheme itself (see below). The above values for $A^{\alpha 1}$ and $A^{\alpha 2}$ do not depend sizably on the set of CEF parameters chosen.

Going from $A^{\alpha 1}$ and $A^{\alpha 2}$ to $B^{\alpha 1}$ and $B^{\alpha 2}$ requires knowledge of the α background elastic constants $C_0^{\alpha 1}$, $C_0^{\alpha 2}$, and $C_0^{\alpha 12}$. Extrapolating values ($C_{11}=25.5$, $C_{33}=31.6$, $C_{11}-C_{12}=16.6$, $C_{44}=4.95$, and $C_{66}=1.7$ in 10^{11} ergs/cm³ units) from the elastic constants measured in HoVO₄ (Ref. 26) and TmPO₄²⁷ and assuming $C_{12}=C_{13}$ in the absence of direct measurements of C_{13} , we deduced $C_0^{\alpha 1}=2.4 \times 10^6$ K, $C_0^{\alpha 2}=1.1 \times 10^6$ K, $C_0^{\alpha 12}=0.16 \times 10^6$ K. This leads to $B^{\alpha 1}=70$ K and $B^{\alpha 2}=-46$ K and then to a magnetoelastic contribution to G^α [Eq. (6')], $G_{ME}^\alpha=4.4$ mK. Using the ratio $K^\mu/G_{ME}^\mu=-1/3$ observed for $\mu=\gamma$ and δ , it may be estimated that G^α is

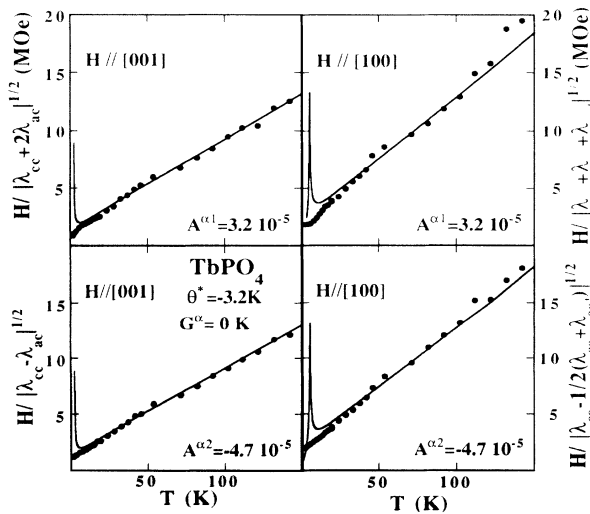


FIG. 4. The temperature variation of the parastriction within the α symmetry for magnetic fields applied along the [001] and [100] axes (upper part: $\alpha 1$ mode; lower part: $\alpha 2$ mode). Curves are calculated with the parameters indicated.

around 3 mK. As the exact values of the B 's and G 's depend on the background elastic constants, to study the feedback of these α quadrupolar terms on the energy and eigenfunction of the levels is possible only qualitatively.

As stated in Sec. II, this α magnetoelastic modulation of the CEF term leads to an apparent second-order CEF coefficient, $\alpha_J V_2^0 = \alpha_J V_2^0 - G^\alpha \langle O_2^0 \rangle$, which is temperature dependent and drives a level "breathing" scheme particularly at low temperature, where the intrinsic quadrupolar moments associated with the Γ_4 singlet ($\langle O_2^0 \rangle \approx 55$) and Γ_5 doublet ($\langle O_2^0 \rangle \approx 22$) are very different. This difference and the close spacing of the two levels are the main reasons for the complexity of the low-temperature phases in TbPO₄. As examples, Fig. 5 (upper part) shows the temperature dependence of $\langle O_2^0 \rangle$ calculated in the presence of the α quadrupolar contributions for set 2. Within the G^α range determined above, the $G^\alpha \langle O_2^0 \rangle$ contribution may be about 10% of the intrinsic CEF term, $\alpha_J V_2^0$. The spacing of the three low-lying levels reflects this α contribution (Fig. 5, lower part): for $G^\alpha=2.5$ mK, the level energies are shifted from their $G^\alpha=0$ values, and the doublet remains the ground state; $G^\alpha=3$ mK is a critical value, which leads to the Γ_4 singlet and Γ_5 doublet being close to each other with the doublet as the ground state between 0.6 and 5.5 K. For $G^\alpha=4$ mK, the singlet is the ground-state owing to its large quadrupolar moment $\langle O_2^0 \rangle$; note that, if not partially canceled by the K^α contribution, for the CEF considered here, $G_{ME}^\alpha=4.4$ mK would drive the Γ_4 singlet to become the ground state.

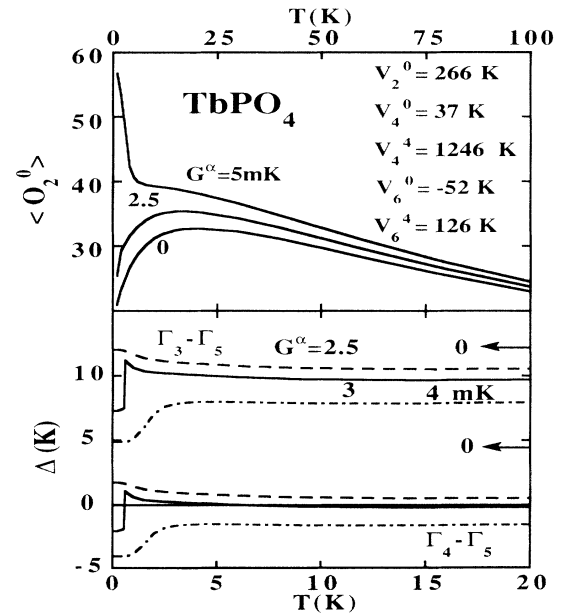


FIG. 5. Upper part: the temperature variation of the $\langle O_2^0 \rangle$ quadrupolar component as a function of the G^α coefficient for the V_1^m parameters indicated. The downward (upward) curvature at low temperature is associated with the Γ_5 doublet (Γ_4 singlet) ground state. Lower part: the corresponding temperature dependence of the low-lying levels (the Γ_3 energy is taken as the reference; the arrows give the temperature-independent energies calculated for $G^\alpha=0$).

In addition to the sizable level “breathing” scheme below 5 K, the main consequence of the α magnetoelastic contributions above 5 K (as soon as the two levels Γ_4 and Γ_5 are both populated), is to introduce an almost temperature-independent shift of the relative energies. Similar behaviors are calculated with the other two sets of V_1^m s. In addition to the measurement of the G^α contribution by parastriction, the determination of the apparent second-order CEF parameter $\alpha_\gamma V_2^0$ by light scattering or neutron spectroscopy could provide us with the actual V_2^0 parameter. This may motivate a neutron spectroscopy experiment at low temperature with a small incident energy (a few meV) in order to study the low-lying level, Γ_5 and Γ_4 as functions of temperature.

This analysis confirms that the low-temperature range (say below 6–7 K) results from the complex coexistence of numerous terms, i.e., the CEF, its α magnetoelastic coupling, bilinear interactions with spin fluctuations in addition to possible external stresses due to the sample mounting, and internal strains due to crystallographic defects, as reported in Ref. 6. This agrees with the “unusually broad and generally asymmetric” lines observed in the absorption spectra collected above 2.3 K as well as with the fact that these lines become sharper in large magnetic fields.⁶ The consequences of a G^α coefficient around 2.5 mK on the various susceptibilities associated with symmetry-lowering modes have been evaluated. This first requires the self-consistent diagonalization of Eq. (1) in the presence of the nonzero G^α coefficient, then the calculation of the single-ion susceptibilities: sizable effects are present only below 5 K. Therefore, to consider these α quadrupolar contributions *ab initio* before calculating the various susceptibilities is not decisive in this study.

In summary, we have obtained clear experimental evidence for the existence of α magnetoelastic couplings in TbPO_4 . The $A^{\alpha 1}$ and $A^{\alpha 2}$ coefficients have been coherently determined. The values of the magnetoelastic coefficients themselves, $B^{\alpha 1}$ and $B^{\alpha 2}$, depend on the background elastic constants, which are not all known: only an estimate of G^α is proposed here, which, fortunately, does not sizably modify the energy and eigenfunctions of the levels and thus the different susceptibilities in the temperature range investigated. This behavior will obviously not be valid when studying the ordered phase.

B. The γ , δ , and ϵ symmetry-lowering modes

The γ -symmetry-lowering mode is obtained from the difference between λ_{aa} and $\lambda_{aa'}$. The negative sign of this difference and the positive value of $\chi_\gamma^{(2)}$ indicate the magnetoelastic coefficient to be negative. The relatively weak value of ϵ^γ limits the temperature range investigated to below 150 K (Fig. 6). The adjustment of the experimental and calculated behaviors leads to $B^\gamma = -100$ K, using $C_0^\gamma = 10^6$ K, an average value in the RVO_4 series ($R = \text{Tb}, \text{Dy}, \text{Ho},$ and Tm).^{1,2,26} Note the change in sign around 4 K calculated for $\chi_\gamma^{(2)}$ is also observed experimentally. This is reminiscent of the α -mode behaviors and the fact that both calculated and observed values agree here is somewhat fortuitous in this complex temperature range.

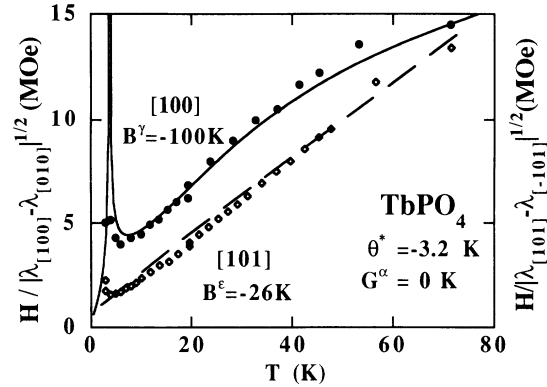


FIG. 6. The temperature variation of the parastriction within the γ ($H \parallel [100]$, data: black dots) and ϵ ($H \parallel [101]$, data: open squares) symmetries. In both cases the changes of length are measured parallel and perpendicular to the field. The lines are calculated with the parameters indicated.

The effects of nonzero G^γ coefficients are significantly reduced due to the weak χ_γ susceptibility. The magnetoelastic contribution to G^γ , $G_{\text{ME}}^\gamma = 10$ mK, is small and does not introduce any significant shift in the parastriction curve.

The $H/|\lambda_{bb} - \lambda_{bb'}|^{1/2}$ values are smaller (Fig. 7) than previously observed at the same temperature for the α and γ modes: this indicates the δ -symmetry-lowering mode is dominant in TbPO_4 . The comparison between the calculated and experimental slopes leads to a positive magnetoelastic coefficient $B^\delta = 145 \pm 7$ K, using a background elastic constant $C_0^\delta = 2.1 \times 10^5$ K, a value estimated as previously from the study of RVO_4 . The magnetoelastic contribution to G^δ reaches $G_{\text{ME}}^\delta = 100 \pm 10$ mK. This large term is mainly driven by the C_0^δ value, which is about five times lower than the C_0^γ one. The gap between calculated and experimental variations corresponds to quadrupolar interactions characterized by $G^\delta = 70 \pm 20$ mK. Here again, one observes that this total coefficient is two thirds of the magnetoelastic contribution. As a gen-

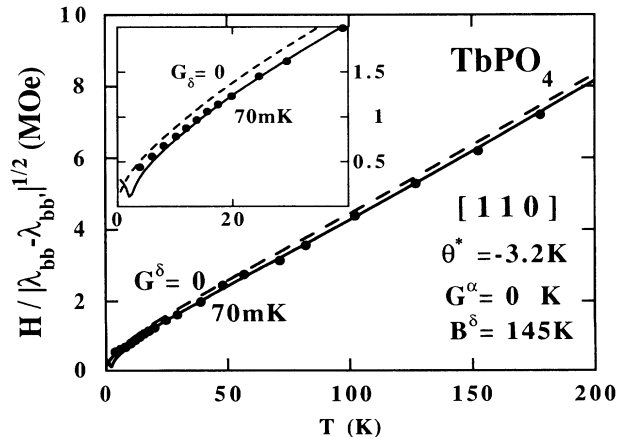


FIG. 7. The temperature variation of the δ parastriction. The full (hatched) lines are calculated with(out) δ quadrupolar interactions. The inset gives the low-temperature behavior.

eral consequence of the large difference between C_0^γ and C_0^δ in R zircons, G^δ is larger than G^γ and the occurrence of a quadrupolar ordering is more frequent for the δ symmetry than for the γ symmetry.

The ε symmetry-lowering mode is usually weak. It does not manifest itself through sizable softenings of the C_{44} elastic constant in the studies devoted to RVO_4 .² Therefore the B^ε magnetoelastic coefficient is generally not determined. However in the case of $TbPO_4$, this mode may be assumed to play an important role in the properties of the ordered phase. Indeed, the tilt of the magnetic moment out from the c axis, which occurs at 2.1 K within the (110) plane,^{10,11} is certainly correlated to the δ quadrupolar interactions, but also involves ε monoclinic magnetoelastic effects. The resulting balance between the different energies may be delicate, and the knowledge of the strength of this last magnetoelastic coupling necessary.

Data have been collected with a magnetic field applied along the [101] axis and gauges along [101] and $[-101]$ in the same way as for the other modes. The difference of the corresponding changes of length at a given temperature leads to $\lambda_{[101]} - \lambda_{[-101]} = 2\sqrt{2}\beta_3\beta_1\varepsilon_1^\varepsilon$. The temperature dependence is then compared to the one calculated in the presence of bilinear interactions (Fig. 6). Comparing the slopes of both variations leads to $B^\varepsilon = -26$ K using a background elastic constant $C_0^\varepsilon = 2C_{44}^0 = 7.8 \times 10^5$ K. This large C_{44}^0 value leads to $G_{ME}^\varepsilon \leq 1$ mK, an effect hidden by experimental uncertainties. Thus this mode is not expected drastically to determine the low-temperature properties.

VI. CONCLUSION

Several points appear from this study. First, our results for the susceptibility are in good agreement with the CEF level scheme determined by Böm, Kahle, and Wüchner.⁶ They also agree with the susceptibility data of Sen, Neogy, and Wanklyn.⁷ It is not possible to select one of the two level schemes proposed by these groups. Generally it is very difficult to determine a unique set of V_1^m parameters in the case of tetragonal symmetry, especially when using a single experimental technique; this is due to the possible vicinity of residue valleys of similar amplitude during fitting, between which the experimental uncertainties do not allow a clear choice. This is a common feature with intermetallics such as $HoAg_2$, for which characteristic behaviors such as changes in sign for the magnetic susceptibility anisotropy and the six transitions seen in neutron-scattering spectra do not lead to an immediate CEF solution.²⁸

An important result is the observation, for the first time to our knowledge, of α magnetoelastic modes, which are determined in two different experimental symmetries. The strengths of the $\alpha 1$ and $\alpha 2$ modes are not negligible by themselves. A similar conclusion seems to arise from studies currently in progress in the RPO_4 series. Whereas the determinations of the $A^{\alpha 1}$ and $A^{\alpha 2}$ coefficients in

$TbPO_4$ are accurate, to determine the $B^{\alpha 1}$ and $B^{\alpha 2}$ magnetoelastic coefficients and thus both the G_{ME}^α contribution and the G^α total quadrupolar parameter requires knowledge of the α elastic constants, which are not all determined in rare-earth zircons. In the case of $TbPO_4$, their consequences for the level scheme are emphasized by the proximity of the first excited level and the ground-state doublet (around 3.6 K): in the presence of the actual CEF parameters, these α magnetoelastic couplings determine the ground state. The thermal dependence at low temperature of the level spacings may be observed by high-resolution neutron spectroscopy using a low incident energy. As a consequence, the low-temperature range, i.e., of the same order of magnitude as the $\Gamma_5 - \Gamma_4$ spacing, appears quite complicated to analyze. In addition, the properties may be very sensitive to stresses resulting from the crystal growth or the sample mounting.

The ε magnetoelastic mode, as the previous α ones, has not been quantitatively evaluated up to now. The $B^\varepsilon = -26$ K coefficient determined in $TbPO_4$ leads to a G_{ME}^ε magnetoelastic coefficient of only 1 mK. Thus we may expect that it plays only a minor role in the magnetic phase diagram below 2.25 K, in particular in the occurrence of the tilt angle for the magnetic moments below 2.15 K.

Along the [100] and [001] axes, the third-order susceptibility is negative, except very close to T_N ; at T_N a rapid increase toward positive values is not driven by quadrupolar interactions, but more probably by short-range order. Such a behavior could also exist along the [110] direction, though hidden by the large positive behavior, explained by δ quadrupolar interactions. Both the third-order susceptibility and parastriction indicate clearly that quadrupolar interactions are dominant within the δ symmetry. The corresponding total coefficient G^δ is determined to be equal to 70 ± 20 mK. The parastriction also provides us with the magnetoelastic coefficient $B^\delta = 145$ K and the magnetoelastic contribution $G_{ME}^\delta = 100 \pm 10$ mK: according to Eq. (6), the K^δ pair interaction coefficient is about -30 mK. Thus the G_{ME}^δ and K^δ values are in agreement with the theoretical ratio, $-1/3$, expected in the case of a dominating acoustic-phonon contribution.^{1,2} Note that, as for the study of the α modes, the susceptibility formalism avoids the determination of the δ coefficients in the very complex low-temperature range.

For the γ symmetry, both parastriction and third-order susceptibility show that the quadrupolar interactions are weakly active; the first reason is the weakness of the γ susceptibilities determined by the CEF in $TbPO_4$; the second one comes from the magnetoelastic characteristics themselves: in spite of a sizable $B^\gamma = -100$ K coefficient, the $G_{ME}^\gamma = 10$ mK value is small due to the elastic constant C_0^γ , which is five times larger than C_0^δ , as is well known in the literature of R zircons.²

All magnetoelastic coefficients have now been determined in $TbPO_4$. In connection with their one-ion origin, they are the strain derivatives of the second-order CEF parameter:¹⁷ $B^\mu = -\alpha_j(\partial V_2^0 / \partial \varepsilon^\mu)$. After normalization

by the second-order Stevens coefficient, they become as characteristic of the series under consideration as the CEF parameters themselves: one is then able to correlate to some degree the magnetoelastic properties in a given system to the properties observed in isomorphous compounds. In TbPO_4 , the following ratios are deduced: $B^\delta/\alpha_J = -14\,400$ K, $B^\gamma/\alpha_J = 9900$ K, $B^\epsilon/\alpha_J = 2600$ K, $B^{a1}/\alpha_J = -7000$ K, and $B^{a2}/\alpha_J = 4600$ K. We have to keep in mind that the last two values are somewhat imprecise due to the fact that some elastic constants are undetermined. None of the magnetoelastic couplings is completely negligible, although the ϵ [shearing within the (100) plane] and α_2 modes (change of the ratio c/a) appear weak. They have to be measured in any thorough study. In comparison with similar variations for magnetoelastic coefficients in cubic intermetallics, the present values relative to the basal plane are clearly larger, contrary to what was claimed in Ref. 17; however, we have to note that the values given in Ref. 17 for some RVO_4 are only estimated and do not result from a fit to measurements as here in the case of TbPO_4 . The question of the origin of the magnetoelastic couplings is identical to the problem of the origin of the CEF itself, which is well known to result from the competition between numerous antagonistic contributions. The problem is still more complicated in the presence of a strain, as the localized charges are displaced from their initial tetragonal arrangement. Such an attempt requires a reliable determination of the different modes across a series, this research is currently underway for the RPO_4 compounds.

A general consequence of the large difference between C_0^γ and C_0^δ in rare-earth zircons is that G^δ is larger than G^γ , and the quadrupolar ordering occurs more frequently for the δ symmetry than for the γ one. Obviously, the occurrence also depends on the susceptibilities determined by the CEF in each compound. Corresponding to the $G^\delta = 70$ mK value observed in TbPO_4 is a quadrupolar order very close to 2.1 K, the temperature at which the reciprocal strain susceptibility diverges in the case of a

second-order process. We have checked that this result does not depend strongly on the exact CEF. Thus TbPO_4 may be understood as dominated by bilinear interactions, characterized by a $\theta^* = -3.2$ K coefficient in the paramagnetic phase, which drives the antiferromagnetic ordering at $T_N = 2.25$ K. The δ quadrupolar interactions then lead to an ordering of the $\langle P_{xy} \rangle$ quadrupolar component at a slightly lower temperature.

However, in this orthorhombic magnetic phase, the magnetic moments have to point in a high-symmetry direction, i.e., the [001] or [110] tetragonal axes. Preliminary calculations by self-consistent diagonalization of the full Hamiltonian [Eq. (1)] with the magnetoelastic coefficients determined here show that the [001] axis remains an easy magnetization direction with a magnetic moment reduced as long as the quadrupolar order exists. The tilt angle observed for the magnetic moment at low temperature would require a G^ϵ coefficient as large as G^δ in order to be described within this model; that is obviously out of the present allowed range. In association with the complex level scheme, which may be sizably temperature dependent in this thermal range due to the α quadrupolar interactions, the low-temperature magnetic phase diagram certainly presents one of the most complex problems one can find in classical magnetism. Thus the present study is just an attempt on which we plan to improve, in particular, by studying magnetoelasticity in the remaining compounds of the series.

ACKNOWLEDGMENTS

The Laboratoire Louis-Néel is Unité Associée à l'Université Joseph-Fourier, Grenoble. This research is supported, in part, by the Russian Fundamental Science Foundation. One of us, Z.K., wants to thank the Ministère de la Recherche et de la Technologie for its support and the Laboratoire Louis-Néel for its hospitality.

-
- ¹G. A. Gerhing and K. A. Gehring, Rep. Prog. Phys. **38**, 1 (1975).
²R. L. Melcher, in *Physical Acoustics*, edited by W. P. Mason and R. N. Thurston (Academic, New York, 1976), Vol. XII, p. 1.
³See, for instance, a comparison of the CEF parameters in HoVO_4 , HoPO_4 , and HoAsO_4 in H. Bischoff, B. Pilawa, A. Kasten, and H. G. Kahle, J. Phys. C **3**, 10057 (1991).
⁴V. I. Sokolov, Z. A. Kazei, and N. P. Kolmakova, Physica B **176**, 101 (1992).
⁵J. F. L. Lewis and G. A. Prinz, Phys. Rev. B **10**, 2892 (1974).
⁶W. Böhm, H. G. Kahle, and W. Wüchner, Phys. Status Solidi B **126**, 381 (1984).
⁷H. Sen, D. Neogy, and B. M. Wanklyn, J. Magn. Magn. Mater. **73**, 221 (1988).
⁸J. N. Lee and H. W. Moos, Phys. Rev. B **5**, 3645 (1972).
⁹G. A. Prinz and J. F. L. Lewis, J. Magn. Magn. Mater. **39**, 285 (1983).
¹⁰J. Coing-Boyat, F. Sayetat, and A. Apostolov, J. Phys. (Paris) **36**, 1165 (1975).
¹¹W. Nägele, D. Holhwein, and G. Domann, Z. Phys. B **39**, 305 (1980).
¹²P. J. Becker, H. G. Kahle, and E. Keller, Phys. Status Solidi B **130**, 191 (1985).
¹³G. Üffinger and A. Kasten, Phys. Status Solidi B **128**, 201 (1985).
¹⁴A. Kasten and G. Üffinger, Phys. Status Solidi B **128**, 525 (1985).
¹⁵S. Bluck and H. G. Kahle, J. Phys. C **21**, 5193 (1988).
¹⁶H. G. Kahle and A. U. Müller, J. Magn. Magn. Mater. **104-107**, 1187 (1992).
¹⁷P. Morin and D. Schmitt, in *Ferromagnetic Materials*, edited by K. H. J. Buschow and E. P. Wohlfarth (North-Holland, Amsterdam, 1990), Vol. 5, p. 1.
¹⁸P. Morin, J. Rouchy, K. Yonenobu, A. Yamagishi, and M. Date, J. Magn. Magn. Mater. **81**, 247 (1989).

- ¹⁹P. Morin and J. Rouchy, *Phys. Rev. B* **48**, 256 (1993).
- ²⁰P. M. Levy, P. Morin, and D. Schmitt, *Phys. Rev. Lett.* **42**, 1417 (1979).
- ²¹K. A. McEwen, U. Steigenberger, and J. L. Martinez, *Physica B* **186**, 371 (1993).
- ²²P. Morin, J. Rouchy, and D. Schmitt, *Phys. Rev. B* **37**, 5401 (1988).
- ²³K. W. H. Stevens, *Proc. Phys. Soc. A* **65**, 209 (1952).
- ²⁴E. du Trémolet de Lacheisserie, *Ann. Phys.* **5**, 267 (1970).
- ²⁵P. Morin, D. Schmitt, and E. du Trémolet de Lacheisserie, *Phys. Rev. B* **21**, 1742 (1980).
- ²⁶T. Goto, A. Tamaki, T. Fujimura, and H. Unoki, *J. Phys. (Japan)* **55**, 1613 (1986).
- ²⁷R. L. Melcher, E. Pytte, and B. A. Scott, *Phys. Rev. Lett.* **15**, 101 (1974).
- ²⁸P. Morin and J. A. Blanco, *J. Magn. Magn. Mater.* **119**, 59 (1993).